

Exact Analytical Equations for Predicting Nonlinear Phase Errors and Jitter in Ring Oscillators

Jaijeet Roychowdhury
jr@ece.umn.edu
University of Minnesota

Abstract

In this paper, we present a simple analytical equation for capturing phase errors in 3-stage ring oscillators. The model, based on a simple but useful idealization of the ring oscillator, is provably exact for small noise perturbations. Despite its simplicity and purely analytical form, our model correctly captures the time-dependent sensitivity of oscillator phase to external perturbations. It is thus well suited for estimating both qualitative and quantitative features of ring oscillator phase response to internal noises, as well as to power, ground and substrate interference. The nonlinear nature of the model makes it suitable for predicting injection locking as well. Comparisons of the new model with existing phase models are provided, and its application for correct prediction of supply-noise induced jitter in PLLs, as well as for capturing injection locking, demonstrated. Requiring knowledge only of the amplitude and frequency of the oscillator, the model is ideally suited for early design exploration at the system and circuit levels. An interesting feature of the analytical equation is its strong connection with the number 1.618034 (the *Golden Mean*), celebrated since ancient times for its significance in a variety of mathematical, aesthetic and scientific disciplines.

1 Introduction

Correct modelling of the phase response of free-running oscillators is of great importance in the design of communication and computer systems. Phase errors caused by device or interference noise result in timing jitter and phase noise; these have a large impact on overall system functionality metrics, such as bit-error rate (BER) in communication systems and clock skew in synchronized digital systems. As a result, it is important to model phase errors as realistically as possible, from the very beginning, during architecture, system and circuit level design.

Indeed, the crucial rôle of *early design exploration* in making overall architectural decisions that best trade off performance vs cost metrics is well recognized by system designers. At the early design stage, only the sketchiest details of each block comprising the system are usually available – typically, only the broad nature or topology of a circuit block will be known. For example, during the early design process, the qualitative phase response properties of ring oscillators might be compared against those of LC oscillators, but the only information available about the oscillator block would be its center frequency and its desired phase noise or jitter performance. Due to the absence of concrete circuit realizations at the early design stage, using *simple generic models* of blocks that, however, capture important qualitative properties correctly, is of the utmost importance.

In this paper, we present a simple analytical equation that captures the phase response of idealized 3-stage ring oscillators

(shown in Figure 1) accurately. The simplicity of the model stems from its explicit dependence on only two design parameters: the amplitude (power) of the output waveforms and the oscillator's desired frequency. The equation is a single scalar nonlinear differential equation for the phase error and is amenable to further simplification and abstraction. Despite its simplicity, the model is powerful enough to capture timing jitter and phase noise due to small device and interference noises accurately. The simple analytical model can also predict injection locking. Existing oscillator phase models for early design (*e.g.*, [9, 12]), which apply a simplistic VCO-like technique of linearly integrating noise/perturbation inputs in time to produce phase errors, do not capture these effects correctly (or at all, *e.g.*, for injection locking).

Our approach is based on a theory for nonlinear perturbation analysis developed in [2, 4], which developed a numerical procedure for finding a periodic phase-sensitivity function, termed the perturbation projection vector or PPV, of any oscillator. In this work, we apply the same rigorous theory, but in a *completely analytical* manner, employing no approximations (other than idealizing the ring oscillator system at the outset). In other words, we start by finding an exact analytical form for the steady-state of the ring oscillator, then obtain its time-varying linearization analytically, and continue to perform Floquet analysis [5] of the system, culminating in expressions for the monodromy matrix [2, 4, 5] and the PPV, analytically. The nonlinear phase macromodel is a simple scalar differential equation that employs this PPV.

Having a simple analytical expression for the PPV (as opposed to a numerical procedure for computing it) has the additional advantage of providing direct design insight into noise and perturbation properties of ring oscillators. The PPV directly captures the time-dependent sensitivity of the oscillator's phase response to any perturbations; hence plots of the PPV, together with knowledge of its scaling properties with respect to oscillation, frequency and amplitude, can guide both circuit and system design decisions without the need for system-level simulation.

Interesting features of our analytical development, at the mathematical level, include Floquet analysis of an impulsive system, a waveform-relaxation-like analytical solution technique, exact analytical eigendecompositions of integer matrices, and a form for the PPV that shows its explicit amplitude- and time-scaling dependence on the frequency/period. An additional curious aspect is that the number $\phi = \frac{1+\sqrt{5}}{2} \simeq 1.618034$, well known as the Golden Mean or Divine Proportion [10, 11], emerges to be central to our exact analytical phase model.

We provide comparisons of the nonlinear equation proposed here with prior linear approaches, in particular the impulse sensitivity function (ISF) based approach of [7]. Extending what has already been shown numerically [2–4] and analytically for

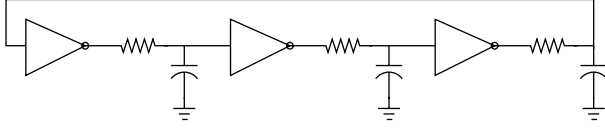


Figure 1: Idealized ring oscillator. The inverters are assumed to switch between output levels of ± 1 , with abrupt switching at input level 0. All resistors/capacitors are assumed identical.

a simple oscillator in radial state space [1], we prove that for the ring oscillator, linear phase equations lead to significant qualitative and quantitative errors. In addition to providing a derivation of the analytical nonlinear phase error equation in Section 2, we provide demonstrations of its application to predicting PLL supply noise induced jitter and injection locking in Section 3.

2 Ring oscillator: analytical perturbation analysis and phase error equations

Figure 1 depicts an idealized 3-stage ring oscillator. All resistors, capacitors and inverters are assumed identical; ideally switching inverters, with output voltages of ± 1 and input switching threshold zero, are assumed. The assumptions of symmetry and zero switching threshold are not essential, having been made simply for convenience; the key assumption, on which much of the following relies, is that of *ideal switching* of the inverters. Deviations from non-ideality (especially delay-related aspects) are captured by the R and C elements outside the inverters.

The key to our novel phase macromodel is that we are able to carry out, in a completely analytical fashion, Floquet analysis [2, 5, 6] of the ring oscillator. Floquet analysis consists solving the linear periodically time-varying (LPTV) system of equations that results from linearizing the nonlinear ring oscillator about its oscillatory steady state. It is important to note, though, that while LPTV calculations are at the core of our procedure, the result of this analysis (a quantity known as the Perturbation Projection Vector, or PPV [2, 4]) is used to form a *nonlinear* macromodel¹. This nonlinearity is key to the accuracy of the analytical equation – for example, for capturing complex dynamical phenomena such as injection locking.

In this section, we obtain the new phase equation via the following steps of Floquet analysis, which we perform analytically:

1. First (Section 2.1), we obtain the differential equations (1) of the ring oscillator of Figure 1.
2. Next (Section 2.2), we find an *exact* analytical oscillatory solution of (1), in terms of the electrical parameters of the circuit. The solution comprises analytical expressions for the time-period T of the oscillator and for the voltage waveforms at the capacitor nodes of Figure 1.
3. Next (Section 2.3), we find the (adjoint) linear periodically time-varying (LPTV) differential equations (13) that capture perturbations to the oscillator around its

¹Indeed, extending LPTV Floquet analysis to capture nonlinear phase behaviour in oscillators is the key qualitative advance of [4] over the prior pioneering work of [8] and related approaches such as [7].

nominal oscillatory steady-state. (13) contains *impulsive terms* due to the abrupt switching of the inverters.

4. Next (Section 2.4), we solve (13) analytically, to obtain a general solution for any initial condition.
5. Using this general solution, we next calculate (Section 2.5) the 3×3 *monodromy matrix* [5, 6] of the oscillator. We find that the entries of the monodromy matrix consist of only the integers 1, 4, 9 and 12. Next, we show that, surprisingly, an exact eigen-analysis of the monodromy matrix is possible *completely analytically*, resulting in expressions for all eigenvalues and eigenvectors. Furthermore, we find that all these quantities are related very simply to a single scalar number, $\varphi = \frac{1+\sqrt{5}}{2} \simeq 1.618034$. Curiously, this quantity is the celebrated *Golden Mean* or *Divine Proportion* (e.g., [10, 11]), a number well known since the days of the ancient Greeks for its significance in fields as diverse as pure mathematics, geometry, science, music and architecture. From the eigenvectors obtained, we choose the eigenvector corresponding to the oscillatory eigenvalue (*i.e.*, Floquet exponent 0).
6. Finally (Section 2.6), we use the general solution of the LPTV equation (13), using the oscillatory eigensolution obtained above, to find the PPV [4] analytically. The analytical expression is found to be a *piecewise-exponential waveform with discontinuities*. With the PPV available analytically, it is embedded within a simple, scalar differential equation [2] to obtain the exact analytical nonlinear phase error macromodel.

2.1 Differential equations for the ring oscillator

From Figure 1, the equations of the ring oscillator may be easily derived from first principles to be

$$\dot{v}_1 = \frac{f(v_3) - v_1}{\tau}, \quad \dot{v}_2 = \frac{f(v_1) - v_2}{\tau}, \quad \dot{v}_3 = \frac{f(v_2) - v_3}{\tau}, \quad (1)$$

where $f(v)$ is the ideal inverter characteristic:

$$f(v) = \begin{cases} -1, & \text{if } v > 0, \\ +1, & \text{otherwise.} \end{cases} \quad (2)$$

Define $\tau = RC$.

2.2 Periodic steady state

Assuming $x(t) = v_1(t)$ is T -periodic, we realize from positive-negative symmetry that

$$x(t) = -(1 + E_0)e^{-\frac{t}{\tau}} + 1, \quad 0 \leq t \leq \frac{T}{2} \quad (3)$$

with $x(0) = -E_0$. Requiring from symmetry that $x(\frac{T}{2}) = E_0$, we obtain

$$\begin{aligned} E_0 &= -(1 + E_0)e^{-\frac{T}{2\tau}} + 1 \\ \Rightarrow E_0(1 + e^{-\frac{T}{2\tau}}) &= 1 - e^{-\frac{T}{2\tau}} \\ \Rightarrow E_0 &= \tanh\left(\frac{T}{4\tau}\right). \end{aligned} \quad (4)$$

From delay symmetry, we have $v_2(t) = x(t - \frac{2T}{3})$ and $v_3(t) = x(t - \frac{T}{3})$. Hence we have

$$0 = -(1 + E_0)e^{-\frac{T}{6\tau}} + 1 \Rightarrow (1 + E_0) = e^{\frac{T}{6\tau}} \Rightarrow \boxed{1 + \tanh\left(\frac{T}{4\tau}\right) = e^{\frac{T}{6\tau}}}; \quad (5)$$

we have

$$\begin{aligned} 2 &= e^{\frac{T}{6\tau}}(1 + e^{-\frac{T}{2\tau}}) \Rightarrow 2 - e^{\frac{T}{6\tau}} - e^{-\frac{T}{6\tau}} = 0 \\ &\Rightarrow 2 - \varphi - \varphi^{-2} = 0, \quad \varphi = e^{\frac{T}{6\tau}} \\ &\Rightarrow \varphi^3 - 2\varphi^2 + 1 = (\varphi - 1)(\varphi^2 - \varphi - 1) = 0. \end{aligned} \quad (6)$$

Solving, we have $\varphi = \frac{1+\sqrt{5}}{2} \simeq 1.6180339889$, the Golden Mean [10]. $T = 6\ln(\varphi)\tau = 2.88727\tau$; close to the 3τ that would result from a perfect delay model. Moreover, $E_0 = \tanh\left(\frac{T}{4\tau}\right) = \tanh\left(\frac{6\ln(\varphi)}{4}\right)$.

Expanding E_0 further in terms of φ , we obtain

$$\begin{aligned} E_0 &= \tanh\left(\frac{6\ln(\varphi)}{4}\right) = \frac{1 - e^{-3\ln(\varphi)}}{1 + e^{-3\ln(\varphi)}} \\ &= \frac{1 - \varphi^{-3}}{1 + \varphi^{-3}} = \frac{\varphi^3 - 1}{\varphi^3 + 1} = \varphi - 1 \simeq 0.6180339889. \end{aligned} \quad (7)$$

Summarizing the periodic steady state waveform of the oscillator, we have:

$$\boxed{\begin{aligned} v_1(t) = x(t) &= \begin{cases} 1 - (1 + E_0)e^{-\frac{t}{\tau}}, & 0 \leq t \leq \frac{T}{2} \\ -1 + (1 + E_0)e^{-\frac{t-T}{\tau}}, & \frac{T}{2} \leq t \leq T \end{cases}, \\ v_2(t) = x(t - \frac{2T}{3}), & \quad v_3(t) = x(t - \frac{T}{3}), \end{aligned}} \quad (8)$$

with $E_0 = \varphi - 1$ and $e^{\frac{T}{\tau}} = \varphi^6$, where $\varphi = \frac{1+\sqrt{5}}{2}$ is the Golden Mean. Denote this periodic steady state by $x_s(t)$, i.e., $x_s(t) = [v_1(t), v_2(t), v_3(t)]^T$. The formula above is confirmed by simulation, as shown in Figure 2.

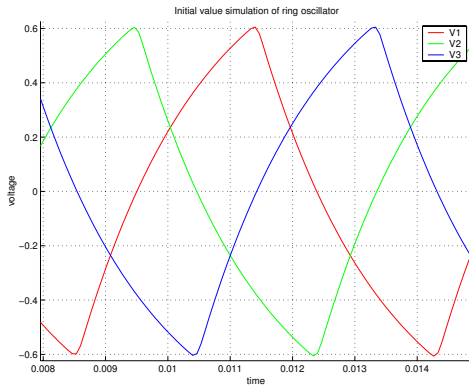


Figure 2: Ring oscillator steady-state waveforms (simulation).

We next obtain an expression for the derivative of $x_s(t)$,

which will be needed later:

$$\begin{aligned} \dot{v}_1(t) = \dot{x}(t) &= \begin{cases} \frac{1}{\tau}(1 + E_0)e^{-\frac{t}{\tau}}, & 0 \leq t \leq \frac{T}{2} \\ -\frac{1}{\tau}(1 + E_0)e^{-\frac{t-T}{\tau}}, & \frac{T}{2} \leq t \leq T \end{cases}, \\ \dot{v}_2(t) = \dot{x}(t - \frac{2T}{3}), & \quad \dot{v}_3(t) = \dot{x}(t - \frac{T}{3}). \end{aligned} \quad (9)$$

In particular,

$$\dot{x}_s(0+) = \frac{1 + E_0}{\tau}[1, a^{-2}, -a^{-1}]^T. \quad (10)$$

2.3 The time-varying linearized system

Next, we need to linearize (1) about the periodic steady state obtained above. Because the inverter characteristic $f(x)$ has a perfect negative step of amplitude 2 at $x = 0$, its derivative is

$$f'(x) = -2\delta(x).$$

From inspection of (1), the forward LPTV system is of the form

$$\dot{y}(t) + G(t)y(t) = 0, \quad (11)$$

where $G(t)$ is a size- 3×3 T -periodic matrix of the form

$$\begin{aligned} G(t) &= \frac{1}{\tau} \begin{bmatrix} 1 & & -f'(v_3(t)) \\ -f'(v_1(t)) & 1 & \\ & -f'(v_2(t)) & 1 \end{bmatrix} \\ &= \frac{1}{\tau} \begin{bmatrix} 1 & & 2\delta(v_3(t)) \\ 2\delta(v_1(t)) & 1 & \\ & 2\delta(v_2(t)) & 1 \end{bmatrix}. \end{aligned} \quad (12)$$

The adjoint system is

$$\dot{y}(t) - G^T(t)y(t) = 0. \quad (13)$$

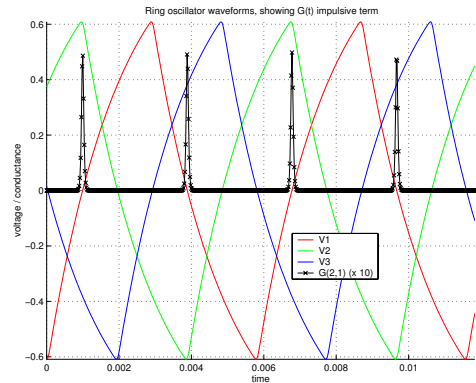


Figure 3: $G_{2,1}(t)$ (simulation)

Recall from the previous section that $v_1(t) = x(t)$; $v_2(t) = x(t - \frac{2}{3}T)$; and $v_3(t) = x(t - \frac{4}{3}T) = x(t - \frac{1}{3}T)$. Hence $v_1(t)$ has a positive zero crossing at $\frac{T}{6}$ and a negative zero crossing at $\frac{2}{3}T$; $v_2(t)$ has a positive zero crossing at $\frac{5}{6}T$ and a negative zero crossing at $\frac{1}{3}T$; and $v_3(t)$ has a positive zero crossing at $\frac{T}{2}$ and a negative zero crossing at 0. Hence we can re-write $G(t)$ as

$$G(t) = \frac{1}{\tau} \begin{bmatrix} 1 & & G_{13}(t) \\ G_{21}(t) & 1 & \\ & G_{32}(t) & 1 \end{bmatrix}, \quad (14)$$

with

$$\begin{aligned} G_{21}(t) &= \frac{2}{|x'(t^*)|} \left(\delta(t - \frac{T}{6}) + \delta(t - \frac{2}{3}T) \right), \\ G_{32}(t) &= \frac{2}{|x'(t^*)|} \left(\delta(t - \frac{5}{6}T) + \delta(t - \frac{1}{3}T) \right), \\ G_{13}(t) &= \frac{2}{|x'(t^*)|} \left(\delta(t) + \delta(t - \frac{T}{2}) \right). \end{aligned} \quad (15)$$

(14) is valid over $t \in [0, T]$, with $G(t)$ T -periodic. $t^* = \frac{T}{6}$ is the point where $x(t)$ crosses zero; the slope at this point is

$$x'(t^*) = \frac{1}{\tau},$$

which follows directly from (1). Incorporating $x'(t^*)$ correctly in (14) is important for capturing the integrals of the δ -function terms, which are key metrics to be preserved. Figure 3 depicts the impulse-like $G_{1,2}(t)$ obtained from simulation. Note that the spikes, synchronized with zero-crossings of $x(t) = v_1(t)$, are all positive, as predicted by (14).

2.4 Solution of the adjoint LPTV system

Noting that

$$G^T(t) = \frac{1}{\tau} \begin{bmatrix} 1 & G_{21}(t) & \\ & 1 & G_{32}(t) \\ G_{13}(t) & & 1 \end{bmatrix}, \quad (16)$$

we can expand the adjoint LPTV system $\dot{z} - G^T(t)z(t) = 0$ into individual components, and denoting $S' = \frac{2}{\tau|x'(t^*)|} = 2$, we obtain

$$\begin{aligned} \dot{z}_1 &= \frac{z_1(\tau)}{\tau} + S' \left(\delta(t - \frac{T}{6})z_2(\frac{T}{6}) + \delta(t - \frac{2}{3}T)z_2(\frac{2}{3}T) \right), \\ \dot{z}_2 &= \frac{z_2(\tau)}{\tau} + S' \left(\delta(t - \frac{1}{3}T)z_3(\frac{1}{3}T) + \delta(t - \frac{5}{6}T)z_3(\frac{5}{6}T) \right), \\ \dot{z}_3 &= \frac{z_3(\tau)}{\tau} + S' \left(\delta(t)z_1(0) + \delta(t - \frac{T}{2})z_1(\frac{T}{2}) \right). \end{aligned} \quad (17)$$

The above equations can be solved analytically, using a waveform-relaxation-like approach, because of the simplicity of integrating δ functions. For given initial conditions $z_1(0)$, $z_2(0)$ and $z_3(0)$, the solution is

$$\begin{aligned} z_1(t) &= \left(z_1(0) + S' \left(e^{-\frac{T}{6\tau}} z_2(\frac{T}{6}) u(t - \frac{T}{6}) + e^{-\frac{2T}{3\tau}} z_2(\frac{2T}{3}) u(t - \frac{2T}{3}) \right) \right) e^{\frac{t}{\tau}} \\ z_2(t) &= \left(z_2(0) + S' \left(e^{-\frac{T}{3\tau}} z_3(\frac{T}{3}) u(t - \frac{T}{3}) + e^{-\frac{5T}{6\tau}} z_3(\frac{5T}{6}) u(t - \frac{5T}{6}) \right) \right) e^{\frac{t}{\tau}}, \\ z_3(t) &= \left(z_3(0) + S' \left(z_1(0) u(t) + e^{-\frac{T}{2\tau}} z_1(\frac{T}{2}) u(t - \frac{T}{2}) \right) \right) e^{\frac{t}{\tau}} \end{aligned} \quad (18)$$

as can be verified by direct substitution.

Observe that the solution is not completely specified yet, since the unknown quantities $z_1(\frac{T}{6})$, $z_2(\frac{T}{6})$, $z_2(\frac{2T}{3})$, $z_3(\frac{T}{3})$ and $z_3(\frac{5T}{6})$ appear on the right hand side of (18). We can, however, solve for these in three passes through (18). In the first pass, we obtain

$$\begin{aligned} z_2(\frac{T}{6}) &= z_2(0) e^{\frac{T}{6\tau}}, \\ z_3(\frac{T}{3}) &= \left(z_3(0) + S' z_1(0) \right) e^{\frac{T}{3\tau}}, \end{aligned} \quad (19)$$

in the second pass, we obtain

$$\begin{aligned} z_1(\frac{T}{2}) &= \left(z_1(0) + S' z_2(0) \right) e^{\frac{T}{2\tau}} \\ z_2(\frac{2T}{3}) &= \left(z_2(0) + S' \left(z_3(0) + S' z_1(0) \right) \right) e^{\frac{2T}{3\tau}}, \end{aligned} \quad (20)$$

and in the third pass, we obtain

$$z_3(\frac{5T}{6}) = \left(z_3(0) + S' \left(2z_1(0) + S' z_2(0) \right) \right) e^{\frac{5T}{6\tau}}. \quad (21)$$

Substituting (19), (20) and (21) in (18), we obtain

$$\begin{aligned} z_1(t) &= \left(z_1(0) + S' \left(z_2(0) u(t - \frac{T}{6}) + z_2(0) + \right. \right. \\ &\quad \left. \left. S' [z_3(0) + S' z_1(0)] u(t - \frac{2T}{3}) \right) \right) e^{\frac{t}{\tau}}, \\ z_2(t) &= \left(z_2(0) + S' \left([z_3(0) + S' z_1(0)] u(t - \frac{T}{3}) \right. \right. \\ &\quad \left. \left. + [z_3(0) + S' (2z_1(0) + S' z_2(0))] u(t - \frac{5T}{6}) \right) \right) e^{\frac{t}{\tau}}, \\ z_3(t) &= \left(z_3(0) + S' \left(z_1(0) u(t) + [z_1(0) + S' z_2(0)] u(t - \frac{T}{2}) \right) \right) e^{\frac{t}{\tau}}, \end{aligned} \quad (22)$$

valid over $t \in [0, T]$.

2.5 Monodromy matrix of the adjoint LPTV system

To obtain the adjoint monodromy matrix, we need to evaluate the above at $t = T$, for initial conditions e_1 , e_2 and e_3 , respectively. Doing so, we obtain

$$M_A = \begin{bmatrix} 1 + S'^3 & 2S' & S'^2 \\ 3S'^2 & 1 + S'^3 & 2S' \\ 2S' & S'^2 & 1 \end{bmatrix} e^{\frac{T}{\tau}}. \quad (23)$$

Recalling that $S' = \frac{2}{\tau|x'(t^*)|} = 2$ and that $e^{\frac{T}{\tau}} = \phi^6$ (where $\phi = \frac{\sqrt{5}+1}{2} \simeq 1.6180$, $\frac{1}{\phi} = \frac{\sqrt{5}-1}{2}$), we have

$$M_A = \underbrace{\begin{bmatrix} 9 & 4 & 4 \\ 12 & 9 & 4 \\ 4 & 4 & 1 \end{bmatrix}}_{M_{Ai}} \phi^6. \quad (24)$$

The characteristic polynomial of M_{Ai} above is

$$p_A(\lambda) = \lambda^3 - 19\lambda^2 + 19\lambda - 1,$$

hence the eigenvalues of M_{Ai} are

$$\lambda_{1,Ai} = \phi^{-6}, \quad \lambda_{2,Ai} = 1, \quad \lambda_{3,Ai} = \phi^6, \quad (25)$$

resulting in eigenvalues for M_A of $\{1, \phi^6, \phi^{12}\}$. (Note that $\phi^6 = 9 + 4\sqrt{5}$ and that $\phi^{-6} = 9 - 4\sqrt{5}$). The eigendecomposition of M_{Ai} is

$$\underbrace{\begin{bmatrix} 9 & 4 & 4 \\ 12 & 9 & 4 \\ 4 & 4 & 1 \end{bmatrix}}_{M_{Ai}} \underbrace{\begin{bmatrix} -\phi^{-1} & -1 & \phi \\ \phi^{-2} & 1 & \phi^2 \\ \phi & 1 & 1 \end{bmatrix}}_V = \underbrace{\begin{bmatrix} -\phi^{-1} & -1 & \phi \\ \phi^{-2} & 1 & \phi^2 \\ \phi & 1 & 1 \end{bmatrix}}_V \underbrace{\begin{bmatrix} \phi^{-6} & & \\ & 1 & \\ & & \phi^6 \end{bmatrix}}_{\Lambda_{Ai}}. \quad (26)$$

Therefore,

$$M_A V = V \Lambda_A, \quad \text{with } \Lambda_A = \begin{bmatrix} 1 & & \\ & \phi^6 & \\ & & \phi^{12} \end{bmatrix}. \quad (27)$$

2.6 Analytical PPV and nonlinear phase macro-model

We are now in a position to obtain an analytical expression for the perturbation projection vector (PPV) [2, 4] of the ring oscillator. Note that the eigenvector $v_1(0)$, corresponding to the periodic Floquet multiplier (eigenvalue 1), is the first column of V , or

$$V_1(0) = \varphi^{-1}[-1, \varphi^{-1}, \varphi]^T. \quad (28)$$

Applying $v_1(0)$ as the initial condition to (22), we obtain the scaled PPV function:

$$\begin{aligned} V_{11}(t) &= \varphi^{-1} \left(-1 + 2 \left(\varphi^{-1} u(t - \frac{T}{6}) + (\varphi^{-1} + 2\varphi - 4) u(t - \frac{2T}{3}) \right) \right) e^{\frac{t}{\tau}}, \\ V_{21}(t) &= \varphi^{-1} \left(\varphi^{-1} + 2 \left([\varphi - 2] u(t - \frac{T}{3}) + [\varphi + 4\varphi^{-1} - 4] u(t - \frac{5T}{6}) \right) \right) e^{\frac{t}{\tau}}, \\ V_{31}(t) &= \varphi^{-1} \left(\varphi + 2 \left(-u(t) + [-1 + 2\varphi^{-1}] u(t - \frac{T}{2}) \right) \right) e^{\frac{t}{\tau}}. \end{aligned} \quad (29)$$

To obtain a properly scaled PPV, we need to normalize (29) against $\dot{x}_s(t)$. It suffices to calculate $K_A = V_1^T(0+) \dot{x}_s(0+)$; however, care is necessary in this calculation, since, from (29), $V_{31}(0) \neq V_{31}(0+)$. Using (10) and (29), we obtain (using $\varphi^{-2} - 2 = -\varphi$ and $E_0 = \frac{\varphi^3 - 1}{\varphi^3 + 1}$)

$$\begin{aligned} K_A &= V_1^T(0+) \dot{x}_s(0+) = \varphi^{-1} \frac{1 + E_0}{\tau} [-1, \varphi^{-1}, \varphi - 2] \cdot [1, \varphi^{-2}, -\varphi^{-1}]^T \\ &= \varphi^{-1} \frac{1 + E_0}{\tau} [-1, \varphi^{-1}, -\varphi^{-2}] \cdot [1, \varphi^{-2}, -\varphi^{-1}]^T \\ &= \varphi^{-1} \frac{1 + E_0}{\tau} (-1 + 2\varphi^{-3}) = \varphi^{-1} \frac{2\varphi^3}{\tau(1 + \varphi^3)} (-1 + 2\varphi^{-3}) \\ &= \varphi^{-1} \frac{2}{\tau} \left(\frac{2 - \varphi^3}{1 + \varphi^3} \right). \end{aligned} \quad (30)$$

We confirm correctness of K_A by also computing it as

$$\begin{aligned} K_A &= V_1^T(0-) \dot{x}_s(0-) = \varphi^{-1} \frac{1 + E_0}{\tau} [-1, \varphi^{-1}, \varphi] \cdot [-\varphi^{-3}, \varphi^{-2}, -\varphi^{-1}]^T \\ &= \varphi^{-1} \frac{1 + E_0}{\tau} (-1 + 2\varphi^{-3}) \end{aligned} \quad (31)$$

and noting that the result is identical to (30).

Applying the scaling constant, we obtain an analytical expression for the PPV of an ideal three-stage ring oscillator:

$$\text{PPV}(t) = \tau \frac{1 + \varphi^3}{4 - 2\varphi^3} \begin{bmatrix} -1 + 2 \left[\varphi^{-1} u(t - \frac{T}{6}) + (\varphi^{-1} + 2\varphi - 4) u(t - \frac{2T}{3}) \right] \\ \varphi^{-1} + 2 \left[(\varphi - 2) u(t - \frac{T}{3}) + (\varphi + 4\varphi^{-1} - 4) u(t - \frac{5T}{6}) \right] \\ \varphi + 2 \left[-u(t) + (-1 + 2\varphi^{-1}) u(t - \frac{T}{2}) \right] \end{bmatrix} e^{\frac{t}{\tau}}. \quad (32)$$

Observe that the three components of the PPV in (32) are simply shifts of a single waveform; hence (32) can be re-written as:

$$\text{PPV}(t) = \begin{bmatrix} \text{PPV}_3(t - \frac{2T}{3}) \\ \text{PPV}_3(t - \frac{T}{3}) \\ \text{PPV}_3(t) \end{bmatrix}, \quad (33)$$

where

$$\begin{aligned} \text{PPV}_3(t) &= \tau \frac{1 + \varphi^3}{4 - 2\varphi^3} \left(\varphi + 2 \left[-u(t) + (-1 + 2\varphi^{-1}) u(t - \frac{T}{2}) \right] \right) e^{\frac{t}{\tau}} \\ &\simeq \tau \left(0.4472 - 0.5528u(t - \frac{T}{2}) \right) e^{\frac{t}{\tau}}. \end{aligned} \quad (34)$$

With the analytical expression for the PPV (34) available, the nonlinear phase macromodel of the ring oscillator can be expressed as [2, 4]

$$\dot{\alpha}(t) = \text{PPV}^T(t + \alpha(t)) \cdot b_p(t), \quad (35)$$

where $\alpha(t)$ is the timing jitter caused by the vector perturbation $b_p(t)$ to the oscillator. The components of $b_p(t)$ represent current injections into the respective nodes of the circuit in Figure 1.

3 Application of the Analytical Phase Model

3.1 Feature comparison against linear phase macromodels

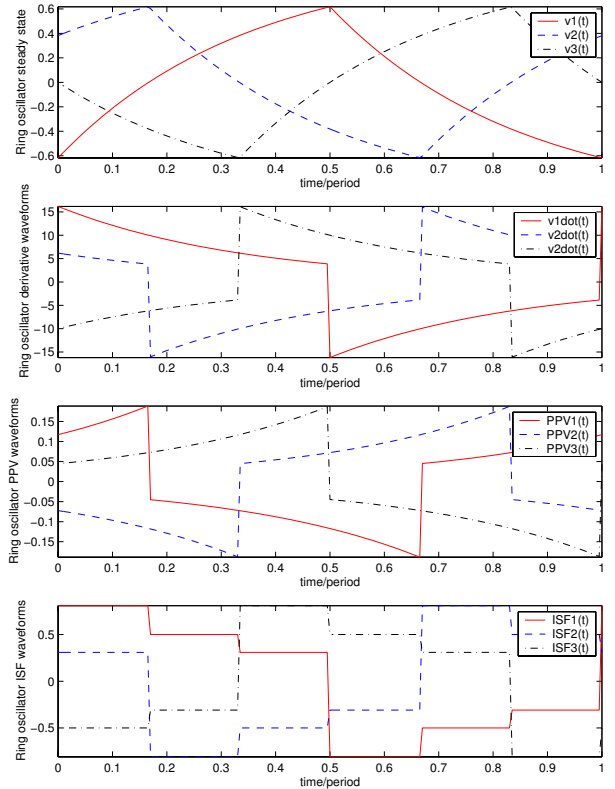


Figure 4: Plots (from analytical expressions) of the steady state waveform, its derivative, the PPV and the ISF [7, Equation 31] of the ideal 3-stage ring oscillator.

Figure 4 plots the PPV (34) for a ring oscillator with $\tau = 0.1$, together with the ring oscillator's steady-state waveform, its derivative, and the impulse-sensitivity function (ISF) from [7, Equation 31] for comparison. Several noteworthy facts about the PPV are evident.

The first interesting feature that the PPV makes apparent is that “jumps” in the PPV component of a given node (e.g., node 1, the solid lines) are not synchronized in any simple manner with the steady-state waveform or its derivative. Indeed, the PPV's discontinuities, which occur at its maxima/minima, take place when the oscillator's response is smooth. This indicates

that any intuition about the phase sensitivity of a ring oscillator that is based on when nodes change rapidly is erroneous. Indeed, the correct intuition, derived from the PPV waveform, is that a node is most sensitive to noise and perturbations when the *prior* node in the ring experiences rapid transitions.

Secondly, it should be noted that although the PPV has a shape similar to the derivative of the steady state, the two are not identical – both time-shifts and amplitudes are different. In fact, from the expressions, it can be seen that the *two waveforms scale in opposite directions* with respect to the RC time constant τ . Hence, intuition about ring oscillator sensitivity that is based on the amplitude and shape of the tangent vector of the oscillator's state-space trajectory is erroneous.

Finally, Figure 4 also depicts the shape of the impulse sensitivity function (ISF) of [7], a concept based on the normalized tangent vector, that has received wide attention amongst the RF and mixed-signal design community. As has already been established [1–4], the theory behind the tangent-vector interpretation of the ISF is incorrect, hence its use can lead to large errors in jitter and phase noise prediction. This is underscored by the dramatically different shape and magnitude of the ISF compared to the PPV, which is the correct measure of the oscillator's time-dependent sensitivity to external perturbations.

While the PPV scales linearly with τ , the ISF, being normalized to 1, does not scale similarly. Phase changes from using the ISF can in fact be of the opposite direction from the correct one. For example, if a noise impulse is injected into node 1 at time about $t = \frac{1}{5}T$ (i.e., 0.2 along the horizontal axis), the ISF predicts a positive phase change, whereas in fact, the correct phase change is in the positive direction (and of a different magnitude), as predicted by the PPV.

4 Conclusion

In this paper, we have presented a nonlinear, completely analytical equation that correctly captures phase errors in 3-stage ring oscillators. We anticipate that this model will be of significant use in guiding ring oscillator design and providing insight not only into random noise, but also for interference, injection locking, *etc.*. We have demonstrated that the equation correctly captures power-supply interference related jitter in PLLs, as well as injection locking. Inaccuracies that can result from the use of earlier models, including time-varying ones, have been clarified. In addition to its intrinsic scientific value, the model, easily encapsulated in MATLAB, is well suited for early design exploration and simulations at the system level.

References

- [1] G. Coram. A Simple 2-D Oscillator to Determine the Correct Decomposition of Perturbations into Amplitude and Phase Noise. IEEE Trans. Ckts. Syst. – I: Fund. Th. Appl., 48:896–898, July 2001.
- [2] A. Demir, A. Mehrotra, and J. Roychowdhury. Phase noise in oscillators: a unifying theory and numerical methods for characterization. IEEE Trans. Ckts. Syst. – I: Fund. Th. Appl., 47:655–674, May 2000.
- [3] A. Demir and J. Roychowdhury. On the validity of orthogonally decomposed perturbations in phase noise analysis. Technical memorandum, Bell Laboratories, Murray Hill, 1997.
- [4] A. Demir and J. Roychowdhury. A Reliable and Efficient Procedure for Oscillator PPV Computation, with Phase Noise Macromodelling Applications. IEEE Trans. Ckts. Syst. – I: Fund. Th. Appl., pages 188–197, February 2003.
- [5] M. Farkas. Periodic Motions. Springer-Verlag, 1994.
- [6] R. Grimshaw. Nonlinear Ordinary Differential Equations. Blackwell Scientific, 1990.
- [7] A. Hajimiri and T.H. Lee. A general theory of phase noise in electrical oscillators. IEEE J. Solid-State Ckts., 33:179–194, February 1998.
- [8] F. Kärtner. Analysis of white and $f^{-\alpha}$ noise in oscillators. International Journal of Circuit Theory and Applications, 18:485–519, 1990.
- [9] M. Gardner. Phase-lock techniques. Wiley, New York, 1979.
- [10] M. Livio. The Golden Ratio: The Story of PHI, the World's Most Astonishing Number. Broadway, 2003.
- [11] M.L. Wright. The Golden Mean. Website: <http://www.vashti.net/mceinc/golden.htm>.
- [12] J. L. Stensby. Phase-locked loops: Theory and applications. CRC Press, New York, 1997.